Opto-Microwave Signal Processing: Up and Down Conversion Techniques

Tibor Berceli
Márk Csörnyei
Budapest University of Technology & Economics
1111 Budapest
Goldmann György tér 3, Hungary

1. Introduction

This application note introduces the concepts of opto-microwave signal processing used in several communication systems today. Emphasis is placed on optical-microwave up- and down conversion techniques.

In today's and future mobile- or local area networks (LAN) there is a need for optically supported network technologies with a few sophisticated central stations serving a big number of quite simple and cheap optical terminals, such as small base-stations in millimeter-wave optical-wireless local multipoint distribution systems (LMDS), computer or CATV networks. The right answer for all of these challenges is the subcarrier modulated optical transmission.

The subcarrier optical data transmission method offers several advantages over the generally applied TDMA (time division multiple access) system. In a TDMA system the transmitters of the stations are operated on a time sharing basis. In the receivers direct optical detection is used. In a high bit rate data communications network a digital signal processing system with complete capacity should be applied both in the transmitters and in the receivers. That is a big disadvantage which limits the future enhancement of the network capacity.
In case of the subcarrier type optical data communications the transmission capacity of the network can be increased by applying new subcarriers, and thus the digital signal processing system can be kept with unchanged bit rate. The transmitters are used in a continuous operation and in the receivers a heterodyne type detection can be applied which provides a lower noise figure. The continuous operation of the transmitters makes possible several connections working at the same time.
The present method used for reception is rather complex and therefore somewhat troublesome because it applies a tuned filter. Utilizing an opto-microwave mixer there is no need for a tuned filter and thus it is suitable for monolithic integration.

1.1. SUBCARRIER TYPE DATA COMMUNICATIONS

The principle of the subcarrier type data communications is presented first. Each transmitter has its own subcarrier frequency (or frequencies); however, the receivers are tuned to make connection with any transmitter. Thus there is no need for switching in the network because the requested connection is established by tuning the receiver to the wanted subcarrier frequency.
To establish a connection between the stations a signaling channel and a central control unit are applied [1], [4]. An individual subcarrier serves for that purpose applying on/off modulation with a low bit rate and time sharing for the transmitters and receivers. A control unit has a photodetector for the reception of the calling signals coming from the transmitters. The control unit emits ringing signals and control signals for the receivers. The control signal contains the information which subcarrier frequency has to be received by the specific receiver.
The block diagram of the transmitter is shown in Fig. 1. The information signal is modulating the subcarrier frequency. The signaling information is transmitted in a similar way. The subcarrier frequency of the signaling channel is the same for all of the transmitters and receivers. That common signaling channel is used on a time sharing basis. However, the subcarrier frequencies of the information channels are different.

Paper presented at the RTO SET Lecture Series on "Optics Microwave Interactions", held in Jouy en Josas, France, 2-3 September 2002; Duisburg, Germany, 5-6 September 2002; Budapest, Hungary, 9-10 September 2002, and published in RTO-EN-028.

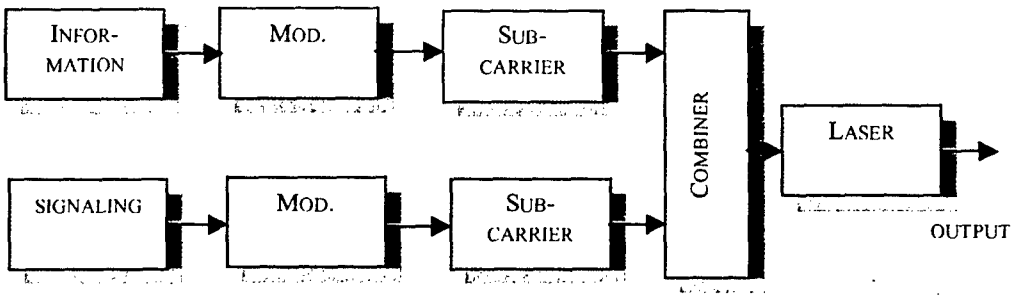

Fig. 1 Block diagram of the transmitter

The block diagram of the receivers is shown in Fig. 2. The received optical signal is detected by a photodiode and the required channel can be selected by a tuned filter. A tuned oscillator is used for further down-conversion. The calling and controlling signals are received in the signaling channel which is transmitted via a fixed frequency subcarrier, and therefore a fixed filter is used in the signaling channel.
As Fig. 2 shows in the conventional direct detection optical receivers there is a need for a tuned filter which makes the high quality realization and MMIC integration quite difficult. Using an opto-microwave mixer in place of the photodetector heterodyne reception scheme can be obtained.

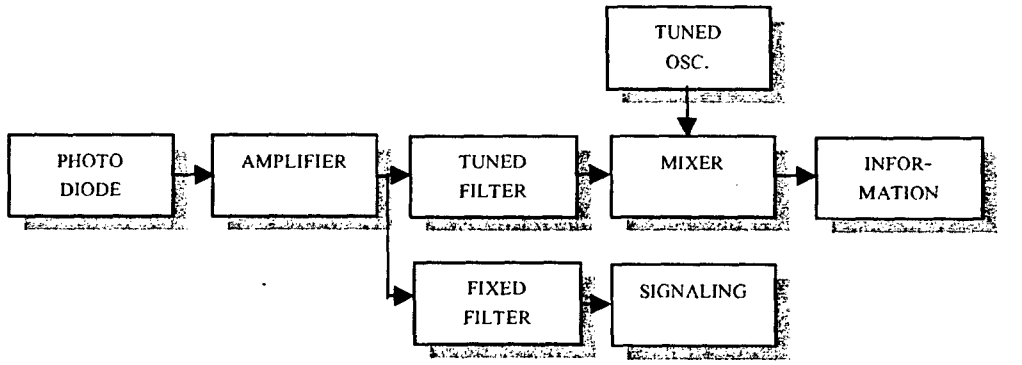

Fig. 2 Block diagram of the receiver

The block diagram of the new receiver is shown in Fig. 3. Instead of a detecting photodiode a mixing device (FET field effect transistor, HEMT high electron mobility transistor, UMZ unbalanced Mach-Zehnder modulator, PIN diode) is used for combined optical-microwave mixing. In such mixers the signal of the tuned local oscillator and the subcarrier of the modulated light are mixed with each other by the device nonlinearities.
The microwave local oscillator is tuned to an off-set frequency of the subcarrier to be received. Thus heterodyne reception is obtained. The unwanted other subcarriers are suppressed by filtering. As seen the new arrangement of Fig. 3 is simpler than the more conventional one of Fig. 2. In the new arrangement there is no tuned filter which is a big advantage.

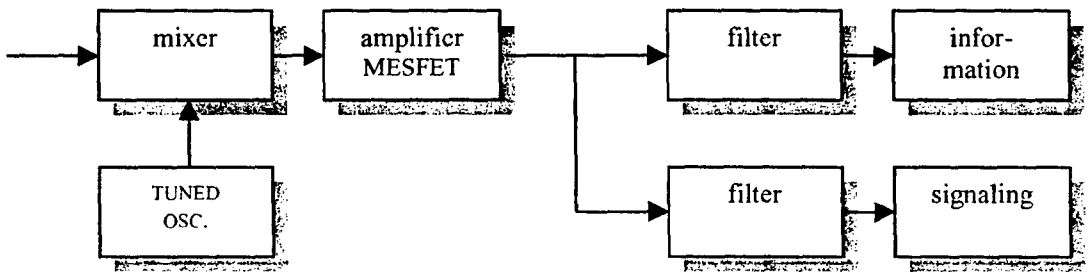

Fig. 3 Block diagram of the receiver with opto-microwave mixer

2. Opto-microwave mixing by MESFETs

This chapter presented here concerns the mixing of a microwave signal with a modulated optical signal in a MESFET. A brief theoretical analysis of the mixing mechanism is given in terms of the input signal parameters and device characteristics. Experimental results for the IF response of the MESFET as a function of RF frequency, incident optical power, optical modulation depth and gate bias voltage are shown.

The basic motivation for the research presented here is the chip-level integration of microwave and photonic components. It is demonstrated that a microwave signal can be mixed with a modulated optical signal in a MESFET, the most commonly used device in MMIC's, for the up- and down-conversion of microwave signals.

2.1. PHOTORESPONSE OF THE MESFET

The following discussion is based on recent work by Malone and Paolella at.al. [1] and [3] related to the internal photovoltaic effect in the MESFET, which gives rise to photoresponse in the device. In the internal photovoltaic effect, illustrated in Fig. 4, the absorbed photons modulate the channel-substrate barrier, thereby modulating the channel height. In effect, the light acts as an "optical gate." We take advantage of this effect to mix an optical signal with a microwave signal in the device.

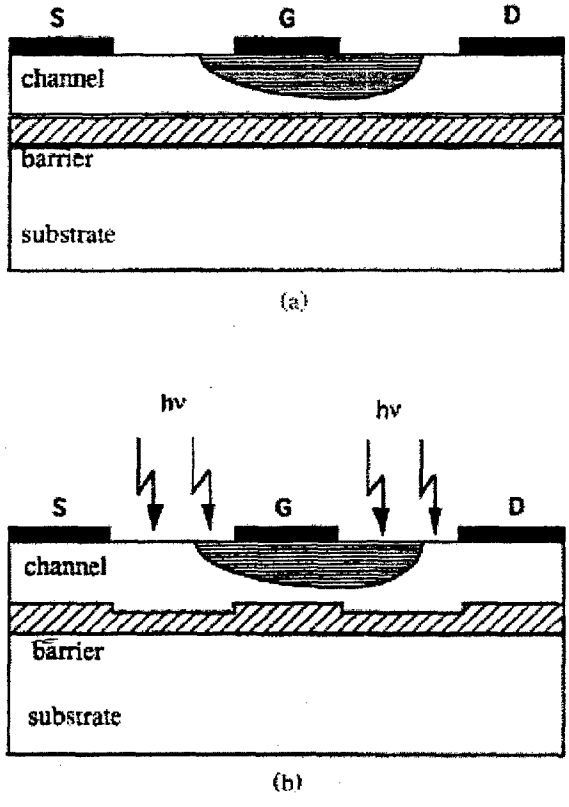

Fig. 4 Internal photovoltaic effect in a GaAs MESFET. The difference in doping level between the epi and substrate layers produces a potential barrier in the standard MESFET, as shown in (a). When illuminated the potential barrier is reduced, as depicted in (b), thereby increasing the channel height (optical gate).

The drain-source current photoresponse for a MESFET was measured as a function of gate-source voltage. The optical signal can be derived from medium power laser operating at 850nm. An optical attenuator controls the power to the MESFET. The optical signal is routed to the MESFET via a cleaved output fiber positioned over the MESFET.

The measured results are presented in Fig. 5. The drain current photoresponse is determined by the measurement of the drain current in the dark and the drain current under illumination, and is expressed as

$$I_{ph} = I_d(\text{illuminated}) - I_d(\text{dark}) \tag{1}$$

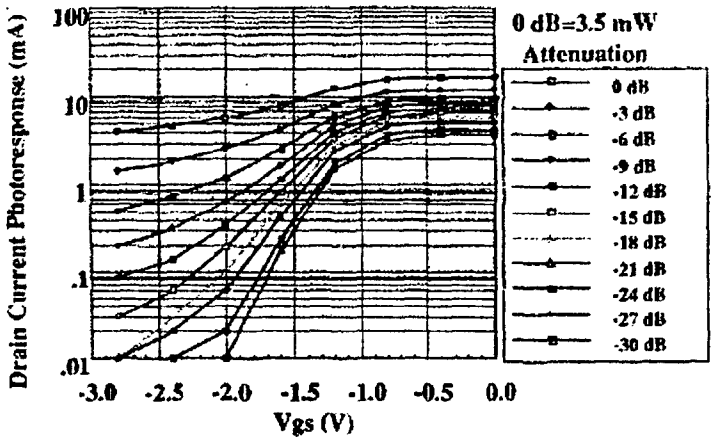

Fig. 5 Drain current photoresponse of the MESFET as a function of gate-source voltage

The photoresponse of the drain current is due to the internal photovoltaic effect and is given as

$$I_{ph} = g_m V_{ph} \tag{2}$$

where g_m is the transconductance of the device. V_{ph} is the optically induced photovoltage[1],[14], which can be written approximately as

$$V_{ph} \approx c_1(L_0)P + c_1 p(L_0)^{(p-1)}(L - L_0) + \ldots \tag{3}$$

where L is the optical intensity, and L_0 is the optical intensity at the operation point. The higher power terms are omitted. The coefficients c_1 and p depend on the specific MESFET. To obtain the coefficients, the photovoltage was measured as a function of optical intensity. The measured relationship was approximated using a curve fitting method.

In Fig. 5 the maximum optical intensity of 3.5mW is used as the 0dB reference, and for each successive curve the intensity is attenuated by 3dB. Under small signal conditions the photoresponse follows the transconductance (g_m) of the device, which is essentially constant with gate bias from 0 to -0.5V. The photoresponse is dominated by the product of the internal photovoltage and g_m when no external resistance is connected to the gate (i.e., R_g=0). As optical intensity is increased, there are contributions to the photoresponse from the substrate photocurrent and the photoconductive current in the channel. The internal photovoltage which is an exponential function will be large resulting in a significant photoresponse well beyond the pinch-off.

2.2. MIXING MECHANISM IN THE MESFET

The mixing effect is the result of the device nonlinearities. In general all elements of the internal equivalent circuit exhibit some nonlinearity, however the dominating factor is the nonlinearity of the drain-source current versus gate-source voltage characteristics. A small effect is obtained from the nonlinear gate-source capacitance as well.

The drain-source current is expressed as a power series of the gate-source voltage at a constant drain-source voltage

$$I_d = I_{db} + a_1 V_{gl} + a_2 (V_{gl})^2 + a_3 (V_{gl})^3 + \ldots \quad (4)$$

where a_1,a_2 and a_3 are coefficients that depend on the drain-source voltage and I_{db} is the dc quiescent point. V_{gl} is the gate-source voltage under illumination.

The effect of illumination on the drain-source current is taken into account by introducing the optically induced photovoltage V_{ph} which is dependent in the light intensity. Thus in case of illumination the gate-source voltage is the sum of the electrically applied voltage and the photovoltage

$$V_{gl} = V_g + V_{ph}. \quad (5)$$

The lightwave illuminating the device is modulated:

$$L = L_0[1 + m\cos(\omega_1 t)] \quad (6)$$

where L_0 is the average optical intensity, and ω_1 and m are the modulation frequency and depth, respectively.

A microwave signal is simultaneously applied across the gate and source

$$V_g = V_{s0}\cos(\omega_2 t) + V_{gb} \quad (7)$$

where V_{s0} is the amplitude, ω_2 is the angular frequency of the microwave signal, t is the time, and V_{gb} is the biasing gate-source voltage.

Thus the gate-source voltage under optical illumination is the sum of the electrically and optically induced voltages

$$V_{gl} = V_{gb} + V_{ph0}\cos(\omega_1 t) + V_{s0}\cos(\omega_2 t) \quad (8)$$

where V_{ph0} is the amplitude of the photovoltage

$$V_{ph0} = c_1 pm(L_0)P. \quad (9)$$

The mixing product in the drain-source current at the intermediate frequency ω_2-ω_1 is obtained by substituting (5) into (4)

$$I_{dmix} = a_2 V_{ph0} V_{s0}. \quad (10)$$

For this result we assume that the second order nonlinear term of (4) is much larger than the higher order terms (i.e. small-signal case). This simplified theoretical derivation shows the dependence of the mixing product in the drain-source current on all the parameters of the microwave input V_{s0}, optical input L_0, and m, as well as the device characteristics, a_2, c_1, and p.

The other nonlinearities of the device can also influence the mixing product; however, their contribution is small. Nevertheless, some effect is obtained from the nonlinearity of the gate-source capacitance. The two signals, i.e. the electrically and the optically induced signals are mixed in the nonlinear gate-source capacitance and then they are amplified due to the transconductance of the device. The capacitive mixing product in the drain-source current is expressed as

$$I_{dmix/cap} = \alpha c_c V_{s0} V_{ph0} / 2 \quad (11)$$

where α is a coefficient presenting the part of the optically induced voltage V_{ph} which effects the gate-source capacitance, and $c_c = \partial C_{gs}/\partial V_g$ being the derivative of the gate-source capacitance with respect to the gate-source voltage. The parameter c_c, represents the part of the photovoltage which influences the gate-to-source capacitance. That influence was measured and a curve fitting method was used to obtain c_c. The parameter α was estimated based on the construction of the FET used. The mixing products in the drain-source current are presented in Fig. 6 based on the measurements performed recently to determine the elements of the MESFET under optical illumination [1]. In Fig. 6 the conversion ratio is plotted with and without capacitive mixing as a function of the gate-source voltage. The conversion ratio is defined as

$$Cr = I_{dmix}/V_{s0}V_{ph0}. \quad (12)$$

As seen in Fig. 6 the contribution of the nonlinear gate-source capacitance is quite small. Some noticeable effect is only observed around the minimum conversion ratio where the drain-source current nonlinearity produces a small mixing product.

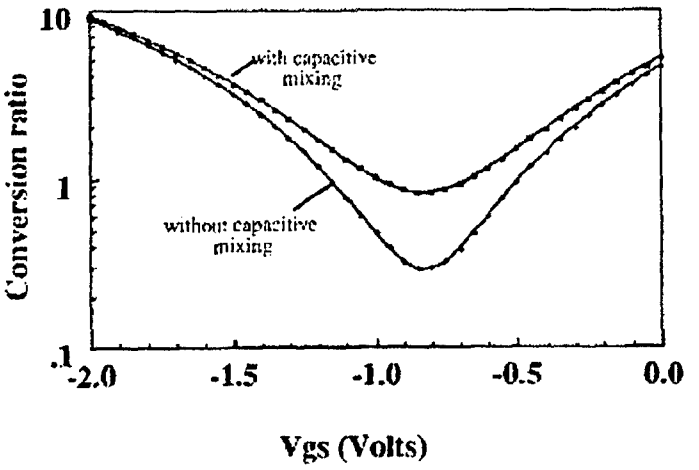

Fig. 6 Conversion ratio as a function of the gate-source voltage with and without capacitive mixing

2.3. COMPARISON OF "DIRECT" AND "INDIRECT" MIXING

There are two basic experimental setups concerning the MESFET as an O/E up- or down-converting front-end in the optical receiver. In an "indirect" mixing configuration (Fig. 7), the MESFET serves as a detector for the optical signal and the up- or down- conversion is performed in a conventional Schottky barrier mixer. However, by taking advantage of the inherent nonlinearities of the MESFET, both detection and frequency conversion of the modulated optical signal can be achieved in the device. This direct mixing approach, shown in Fig.8, is in the focus of this note.

In both of the setups of Fig. 7 and 8 an 850nm wavelength laser can be used. This wavelength is defined by the photosensitivity of the GaAs. The light is directly modulated by the RF Source 1 and positioned on the gate fingers of the MESFET. In case of commonly used microwave transistors, the device should operate with a reverse bias, for example with 0.5 volt at the gate and a drain-to-source voltage of 2 volts. As shown in eq. 9 and 10, the IF or the upconverted term of the drain current is dependent on the optical modulation depth m.

For the indirect mixing configuration, shown in Fig. 7, the MESFET was used as an optical detector. The detected signal from the MESFET was mixed with the signal from RF Source 2 in an additional mixer. As a baseline of comparison, indirect mixing can also be accomplished with a PIN photodetector in place of the MESFET (the conventional optical detection followed by microwave mixing).

For the direct mixing configuration, in addition to the optical input, a signal from RF Source 2 was applied to the gate of the device and the IF output was measured at the drain using a spectrum analyzer with an appropriate resolution.

2.4. EXPERIMENTAL MIXING RESULTS

As an example there are some experimental mixing results for direct mixing with MESFET as an opto-microwave mixer and for indirect mixing accomplished with p-i-n photodetector and a Schottky barrier mixer. The MESFET in the example [1] is an ITT GTC213-1 with four 75μm wide gate fingers, a gate length of 0.8μm and a dopant concentration of $3x10^{17}$ cm^{-3}. The device was operated with a reverse bias. For the direct mixing approach, the signal from an 850nm wavelength laser with an 8GHz bandwidth was directly modulated by an RF source and conveyed to the MESFET by an optical fiber. To maximize the IF response, 100% modulation depth was used on the laser, which has an average optical output power of 1.8mW.

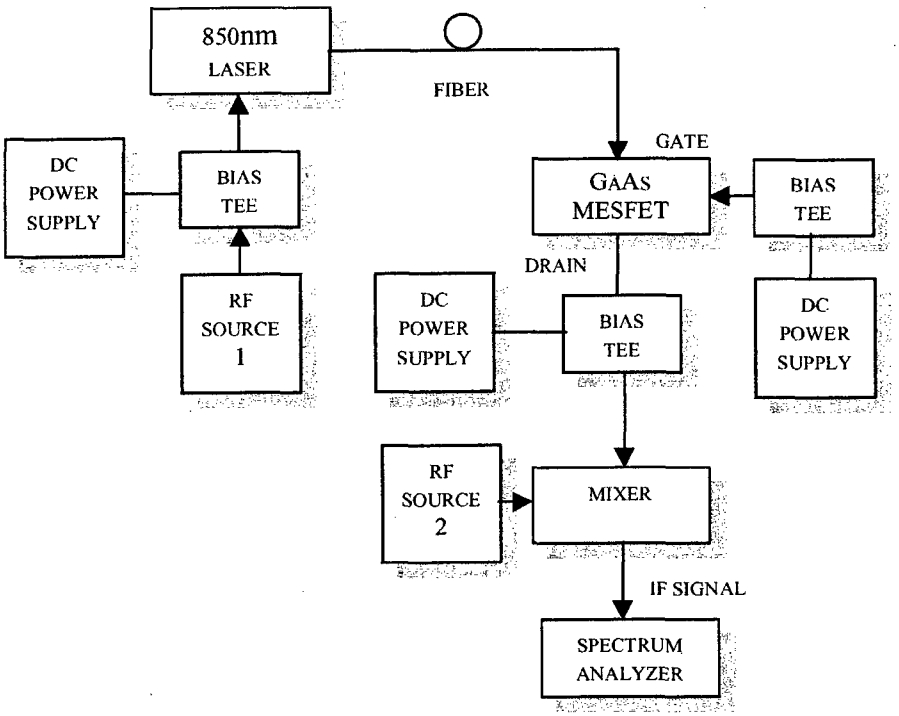

Fig. 7 Indirect mixing configuration

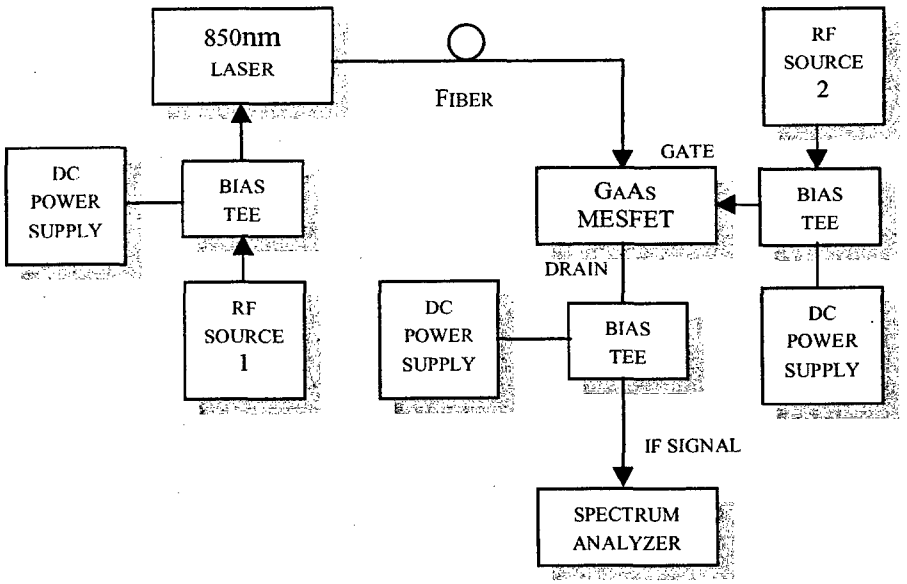

Fig. 8. Direct mixing configuration

The results of optical mixing with MESFET and the conventional detection and mixing with a p-i-n diode and an additional mixer are depicted in Fig. 9. The p-i-n photodetector had a 10GHz bandwidth, a responsivity of 35mA/mW and a diameter of 25μm. The p-i-n operates in this example with a reverse bias of 8V.

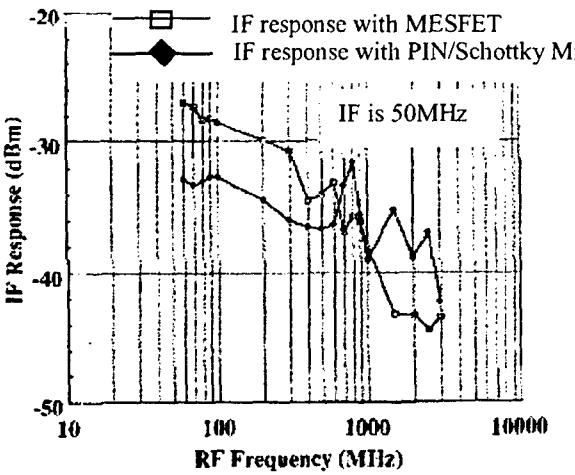

Fig. 9 IF response of the two mixing configurations

In that results of [1] IF response of the MESFET exceeds that of p-i-n/Schottky mixer combination up to an RF frequency of about 700MHz. The IF response emulates the photoresponse spectrum of the device with a conversion loss in range of 7-11dB. Under the same conditions the Schottky mixer had a conversion loss in the range of 4-10dB (See Fig.10). Clearly, as these results show, the MESFET can be used as mixer with optical and microwave inputs. Depending upon the particular application, the data may be an optical signal and the local oscillator an electrical signal, or vice versa.

The dependence of the IF response of the device on the average incident optical power and the RF drive power to the laser is shown in Fig. 11. The slope of the lines indicates that a 1dB decrease in optical power incident on the device translates into a 2dB decrease in the IF response, as expected with square law behavior. The figure also indicates that the IF response decreases linearly with RF drive power to the laser (modulation depth). The conversion response of the MESFET is also strongly dependent on the gate bias voltage. A plot of the IF response versus source-gate voltage at various RF frequencies is shown in Fig. 12. The IF response is maximized when the gate is reverse biased at around 0.5V, which is also the bias voltage at which the transconductance of the device is maximized. Larger reverse bias voltage on the gate decreases the IF response significantly due to a reduction in the gain. However, at bias voltages larger than 1.8V the IF response increases again. This is most likely due to the voltage dependence of the nonlinear coefficient a_2.

The system noise figure is presented in Fig. 13 as a function of the RF frequency. In the figure 3 curves are plotted: one for the p-i-n/Schottky mixer configuration and two for the MESFET with different bias voltages. The noise is significantly smaller with a bias voltage close to pinch-off because then the drain-source current is also smaller. As seen the system noise figure below 1000MHz is smaller in the case of the MESFET than with the p-i-n/Schottky mixer configuration if a bias voltage close to pinch-off is used. However, the system noise figure above 1000MHz is higher in the case of the MESFET compared to the p-i-n/Schottky mixer setup.

2.5. COMPARISON OF DYNAMIC PROPERTIES OF DETECTION AND MIXING, BY FET DEVICES

According to the detection measurements of Berceli et.al. [5] by FET devices, the detected signal exhibits a decay with increasing modulation frequency. The decay is relatively slow at low modulation frequencies. The measurement result is in accordance with the recently published theoretical and experimental investigations.

The decrease in the detected signal with increasing modulation frequency is due to the time constant of the barrier depletion region between the substrate and the epitaxial layer.

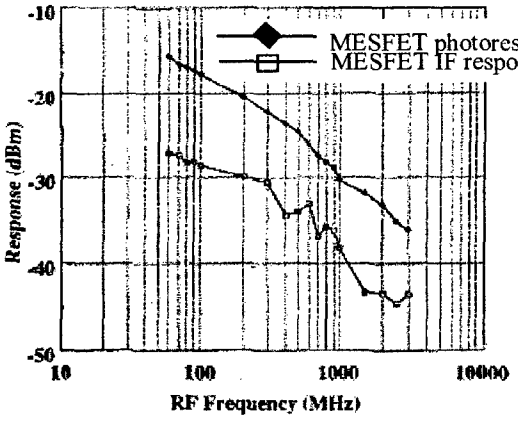

Fig. 10 Photo- and IF response of the MESFET

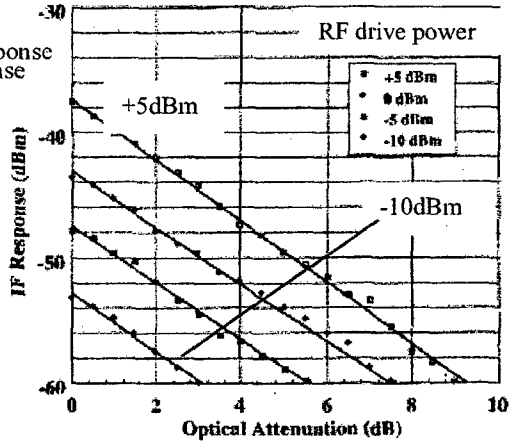

Fig. 11 IF response of the MESFET versus optical attenuation at various RF drive levels. The incedent optical power to the MESFET is 1.8mW.

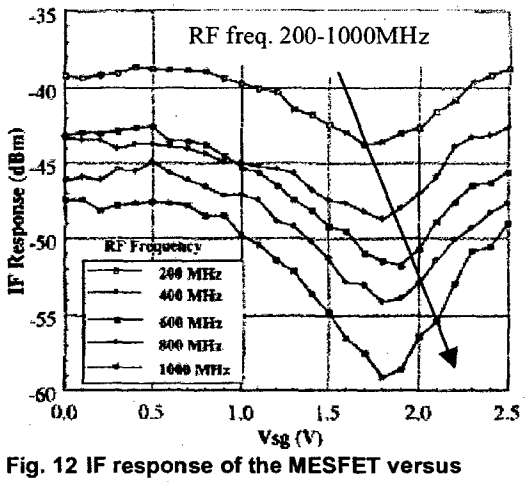

Fig. 12 IF response of the MESFET versus source-gate voltage

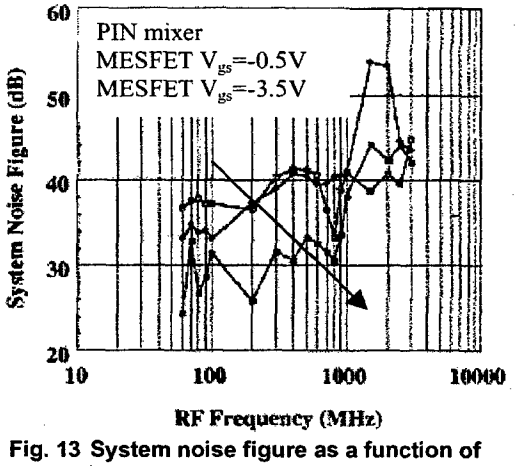

Fig. 13 System noise figure as a function of the RF frequency

The next question is whether the dynamic properties in the detection mode and in the conversion mode of operation are the same.
In the tests investigating the dynamic properties of opto-microwave mixing by FET's, both the optical and microwave gates are driven by signals. Between the gate and source a microwave signal is applied while the intensity modulated signal of a semiconductor laser diode is used to illuminate the active device. The frequency dependence is different, the decay in the converted signal is much higher at low modulation frequencies, and it is more pronounced with increasing modulation frequency compared to the frequency response of the detected signal.
Another significant deviation is that the decrease in the converted signal is proportional to modulation frequency, however, the decrease in the detected signal is developed slowly when the modulation frequency in increasing. The reason of the differences in the dynamic characteristics is the following.
In the detection mode of operation the optically generated charge carriers are contributing to the detected electric current in both depletion regions below the gate and between the substrate and the epitaxial layer by changing the height of the conductive channel. Beside that effect the charge carriers generated in the substrate are also participating in the detected current. Therefore, the frequency dependence of the detected signal is determined by the conductive channel and the substrate currents.
On the other hand, in the mixing mode of operation the contribution of the substrate current in the generation of the mixing product is negligible because in the substrate there is neither a nonlinear nor a parametric effect. The mixing products are created mainly in the conductive channel. This way their power level is somewhat lower and their frequency dependence is higher. There are two reasons for it: the time constant exhibited by the depletion region between the substrate and the epitaxial layer and optically induced substrate current which is increasing with the modulation frequency and doesn't contribute to the mixing effect.

2.6. SINGLE SIDEBAND OPTICAL-MICROWAVE MIXERS

As mentioned in section 2.2 the mixing product in the drain-source current at the difference of the input frequencies (ω_2-ω_1) is:

$$I_{dmix-} = a_2 V_{ph0} V_{s0} \tag{13}$$

The mixing product in the drain-source current at the sum of the input frequencies (ω_1+ω_2) is obtained as follows [4]:

$$I_{dmix+} = a_2 V_{ph0} V_{s0}^{*} \tag{14}$$

V_{s0} is the complex amplitude and V_{s0}^{*} is the conjugate of the complex amplitude of the microwave signal applied across the gate and source. V_{ph0} is the amplitude of the photovoltage.
Comparing these equations it can be seen that there is a phase difference between the mixing product current amplitudes I_{dmix-} and I_{dmix+} because of the conjugation of the microwave signal amplitude in the second case. That makes possible to construct a single sideband optical-microwave mixer arrangement if two mixers are applied in the two branches of a hybrid and 90° phase difference is established between the outputs of the hybrid driving the mixers by the microwave signal. Due to the conjugation of the microwave signal the mixers will provide 180° phase shift in the mixing product current amplitudes which makes possible their separation by another hybrid. A switch is used for choosing the right mixing product for further signal processing.
The principle of the single sideband optical-microwave mixer is presented in Fig. 14, [4].
For the subcarrier type signal reception an important requirement is the high suppression of the image frequency. This is achieved if the mixing products in the two branches are of equal amplitude with a 180° phase difference. However, both the amplitude and the phase of the mixing product are frequency dependent.

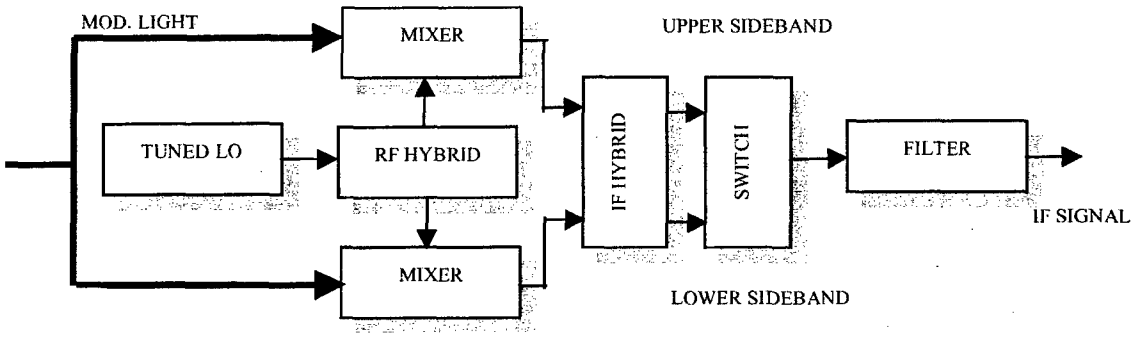

Fig. 14 Block diagram of the new single sideband optical-microwave mixer

3. Optical-microwave double mixing by PIN diodes

The commonly used optical receivers apply mainly photo-diodes to detect the optical intensity modulated signal. A relatively high sensitivity is achieved by properly matched transimpedance or distributed amplifiers.
In another method the modulated optical signal is mixed with a microwave signal in the photodiode producing an intermediate frequency signal. Thus, heterodyne type reception is feasible. However the mixing conversion has a higher loss compared to the direct detection.
In the double optical microwave mixing approach the conversion loss is much less than that of direct detection offering a significant improvement in the reception sensitivity. The mixing product is even further increased by resonance enhancement providing 20dB improvement in comparison to direct detection.

3.1. DOUBLE MIXING PRINCIPLE

This method of Berceli and Járó [7] utilizes simultaneously two effects: a direct and an indirect mixing of the modulated optical signal and the microwave local oscillator signal. For direct mixing the bias is chosen close to the zero voltage where the photo current is highly dependent on both the illumination intensity and applied voltage. Therefore the mixing product is high. At the same time a detection of the optical signal is also obtained which produces a detected signal in the base band. If this signal is reflected back to the photodiode it will also be mixed with the microwave local oscillator signal. Thus the output signal is the resultant of two mixing procedures: an optical-microwave and an electrical mixing (after optical detection).
The double mixing approach [7] is experimentally presented utilizing a 1A358 type CATV p-i-n photodiode. The setup of optical-microwave circuit is shown in Fig. 15.

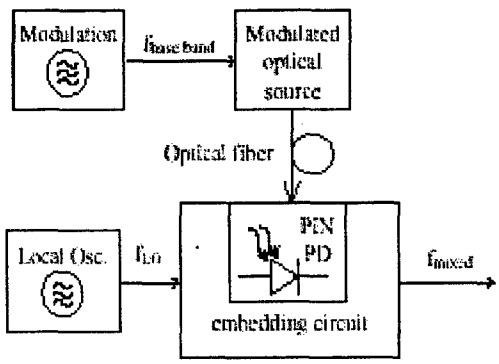

Fig. 15 Optical-microwave mixing setup

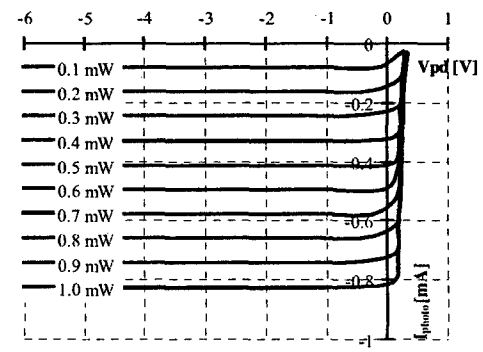

Fig.16 Measured DC characteristic of the pin photodiode

The embedding circuit can be optimized for detection or mixing. The dc characteristics of the p-i-n photodiode is shown in Fig. 16. Here the detected photocurrent is plotted as a function of the bias voltage for different illumination intensities. As seen close to the zero voltage bias point the curvature of the characteristics exhibits a maximum. At this bias voltage the dependence of the photo-current on the light intensity is also maximal. This coincidence ensures the high mixing product in the double mixing approach.The p-i-n photodiode is embedded into a microwave circuit where the detected base band signal is reflected. The photo diode is driven by a microwave local oscillator signal and at the same time it is illuminated by an intensity modulated optical signal. The result is presented in Fig. 17.
Here the mixing product is depicted as a function of the bias voltage. The frequency of the applied local oscillator was 3GHz and the modulation frequency of the intensity modulated optical signal was 540MHz. As seen, about 10dB mixing gain can be achieved biasing the photodiode close to zero voltage.

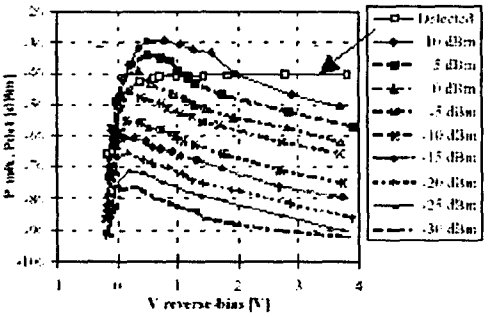

Fig.17 Measured power level of the upconverted signal versus the reverse bias voltage (parameter is the LO power)

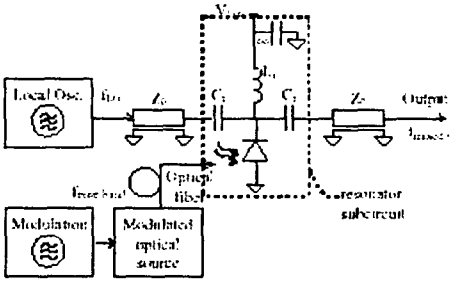

Fig. 18 Measuremtn setup for resonant mixing using a "transmission setup"

3.2. RESONANT ENHANCEMENT

For further improvement the resonant enhancement method can be utilized. The base band and the microwave band are separated by a branching filter as shown in Fig. 18. The reflection in the base band can be adjusted using a sliding short circuit (varying inductance). This way the mixing product is enhanced in a narrow band. The spectrum of the upconverted signal is plotted in Fig. 19.
In the investigations by [7], the frequency of the local oscillator is 2GHz, the photodiode is biased at –0.2V and the series capacitor is 4.7pF. With these settings there is a resonant peak around 50MHz as shown in the figure.

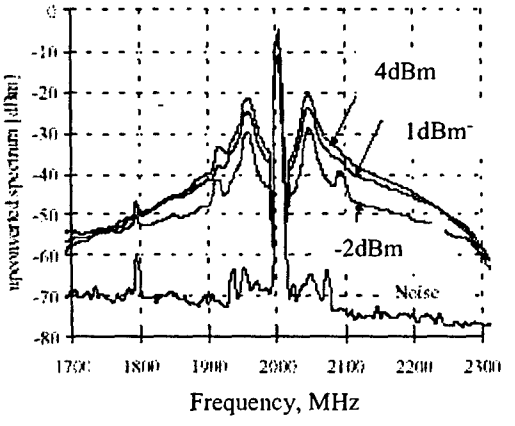

Fig. 19 Measured power level of the upconverted signal (parameter is the LO power) (transmission setup)

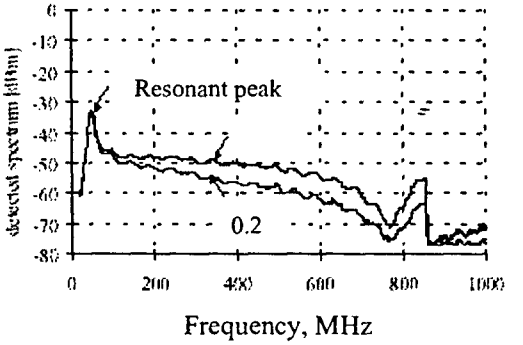

Fig. 20 Measured power level of the detected sigal in resonant condition (parameter is the reverse bias voltage)

The resonance can be measured at base band too. The measured detected spectrum at base band is shown in Fig. 20 at different bias voltages. The peak of the detected spectrum is only an attenuated signal after the series capacitor of the resonator. For comparison Fig. 21 shows the upconverted spectrum using the same configuration setup without resonator subcircuit. In this case the embedding circuit was optimized for detection. Comparing the curves of the Fig. 19 and 21 the effect of the resonance can be seen.

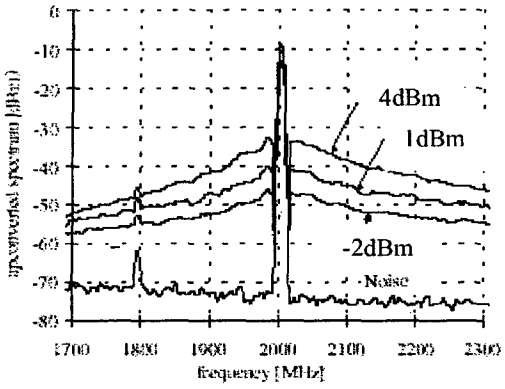

Fig. 21 Measured power level of the upconverted signal without resonator (parameter is the LO power)

4. Frequency conversion methodes by optical interferometer and photodiode

According to [10], there is a comparison of the performance of two different optoelectronic configuration, both used for frequency conversion in the microwave frequency range. In the firs case, mixing is achieved by a Mach-Zehnder (MZ) interferometer, while in the second case, photodiode mixing is presented.

4.1. MIXING WITH UMZ/PD

In the firs case, the optical system used for microwave mixing is a distributed feedback (DFB) laser diode (LD) directly modulated by two microwave frequencies, f_1 (f_{LO} corresponding to the LO signal) and f_2 (in this case, f_{RF}) followed by an unbalanced MZ (UMZ) and a photodetector (PD). The system is shown in the upper portion of Fig. 22.

The basic principle is the nonlinear (sinusoidal) intensity response of the UMZ interferometer/PD combination as a function of the frequency of the optical field. Direct modulation generates FM, which is then converted to AM using the UMZ interferometer working in the coherent regime. The PD detects the optical intensity which is a quadratic function of the optical field, so frequency mixing is obtained. The originality of this solution is the use of a passive optical device inserted in the optical link which generates mixing with better conversion than classical solutions using active MZ modulators.

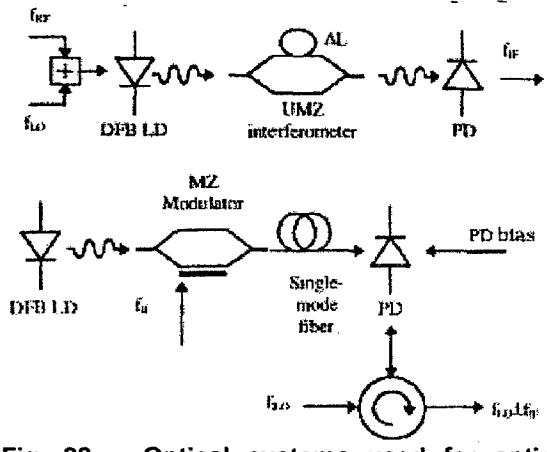

Fig. 22 Optical systems used for optical-microwave mixing

Considering a linear LD operating regime and neglecting AM, the intensity at the output of the interferometer, with delay time τ between both arms is given by

$$I(t)=\frac{E_0^2}{2}\left\{1+V(\tau)\cos\left[2\pi\nu_0\tau+\beta_1\sin\left(\omega_1\frac{\tau}{2}\right)\cdot\cos\left(\omega_1\left(t+\frac{\tau}{2}\right)\right)+\beta_2\sin\left(\omega_2\frac{\tau}{2}\right)\cdot\cos\left(\omega_2\left(t+\frac{\tau}{2}\right)\right)\right]\right\} \quad (15)$$

where $\beta_{1,2}$ is the FM index, $\omega_{1,2}$ is the angular modulation frequency, and $V(\tau)$ reflects the loss of choerence between electric field in both arms of the interferometer. In the coherent working regime $V(\tau)=1$ and in the incoherent regime $V(\tau)=0$. As can be deduced from the equation, in the coherent working regime, when the interferometer is balanced on bright or dark fringe, i.e., when $\cos(2\pi\nu_0 t)=\pm 1$ (condition 1), the rsulting intensity is generated at harmonics and intermodulation products of even order, and in particular, at the mixing frequency f_{IF}. Condition 1 is then the first condition to obtain the best mixing at frequency f_{IF}.

To be optimized, the output spectrum of the optical intensity must exhibit the maximum power of the mixing frequency and the minimum power of the input frequencies. This second condition (condition 2) is fulfilled when

$$f_1=(2k+1)\frac{FSR}{2} \quad (16)$$

and

$$f_2=(2k'+1)\frac{FSR}{2},(k,k')\in N^2 \quad (17)$$

where $FSR=1/\tau=c/(n_{eff}\Delta L)$. Therefore, f_2-f_1 must be as close as possible to a multiple of the free spectral range (FSR). For given input microwave frequencies, the ΔL must be chosen to match these two conditions.

The response at the PD output is periodic with the input frequencies, which means that the device does not optimally work for all frequencies but for particular frequencies in any frequency range. Within a period, the 3dB bandwidth approximates FSR/2. However, in some applications, it is advantageous since the UMZ acts as a microwave filter too.

4.2. PRINCIPLE OF OPTICAL-MICROWAVE MIXING BY PHOTODIODES

The optoelectronic system explored for opto-microwave mixing is shown below the UMZ/PD system in Fig. 22. The mixing was analyzed based on the dc characteristics at different optical intensities illuminating the device. To achieve good detection, the PD is used in its linear regime where the applied reverse bias is usually several volts. However, even in this regime a noticeable nonlinearity is present at higher light injection levels. Simultaneously injecting a microwave signal at the electrical port of the PD and a modulated optical signal results in the mixing of the two signals. The optimal bias points for efficient mixing and for efficient detection are significantly different. The mixing process is explained as a result of the nonlinearity of the PD current-voltage relationship. Due to the fact that the characteristics exhibit the maximum nonlinearity in the vicinity of 0V, it is the optimal operation point for efficient mixing. Nonlinearity of the PD generates several mixing products of the microwave driving signal f_{LO} and of the photo-induced signal f_{IF}. By injecting an LO signal $f_{LO}>f_{IF}$, the detected optical signal is upconverted.

Fig. 23 represents the voltage dependence of the detection and of the mixing products at $f_{LO}+f_{IF}$. In this experiment, f_{LO}=3GHz was used and the light was intensity modulated by f_{IF}=150MHz. Optimal detection is achieved by high reverse bias and a plateau is observed at bias points $V_{PD}<0$. In the absence of electrical excitation, the power of the second harmonic was considerably small, taken into account also the contribution of the modulator part. However, the most efficient mixing is obtained at a bias close to V_{PD}=+0.3V, having a sharp optimum. Conversion loss of the electro-optical mixing process is defined as the ratio of the power at f_{IF} (using the PD in its linear regime as a PD) and of the signal levels at $f_{LO}\pm f_{IF}$ frequencies upconverted by the PD nonlinearity.

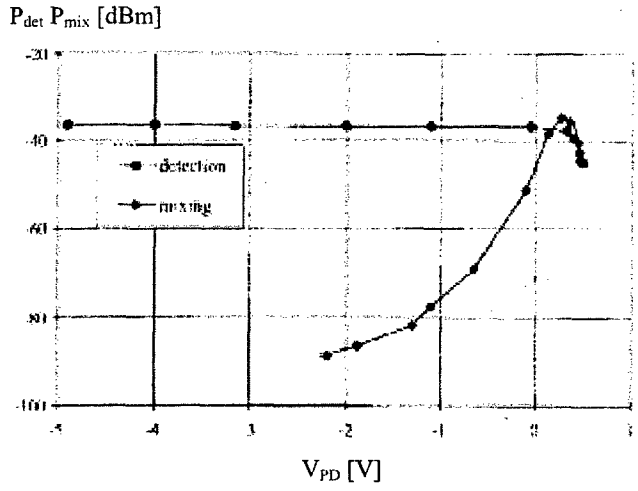

Fig. 23 Voltage dependence of the detected power and of the upper-sideband mixing product.

4.3. EXPERIMENTAL RESULTS WITH UMZ/PD

Measurements were made in [10] with a DFB LD emitting at λ=1300nm, having an I_{th}=13mA and a maximal oscillation frequency of 2.5GHz. The dc-bias current was 22mA and the optical power coupled in the interferometer was 420µW.

To operate in the coherent regime as wanted, the UMZ was realized using only two connectorized –3dB fiber directional couplers. In this case, ΔL=1.6cm, which corresponds to FSR=13GHz.

The LO frequency was F_{LO}=1.9GHz, with a power of –4dBm. The other modulation frequency, f_{RF} was swept from 2 to 2.5GHz and had a power of –18dBm. Fig. 24 shows the power spectrum of the intensity detected by the PD and measured by a spectrum analyzer. In Fig. 24, the lower sideband of the mixing product, f_{LO}-f_{RF}, as well as the third order intermodulation product, was significantly increased by inserting the UMZ. However, the input frequencies f_{LO} and f_{RF} are not rejected. In fact, to obtain an optimal rejection of the fundamentals, condition 1 should first be fulfilled, which was not the case under the conditions of operation. The relative optical phase shift between the two arms is very sensitive to ambient variations, and during the experiments the operating regime continuously varies between minimum and maximum transmission including the quadrature. Secondly, the closer f_I would be to FSR/2=6.5GHz, the larger the rejection would be, and here f_I=f_{LO}=1.9GHz (limitation due to the LD)

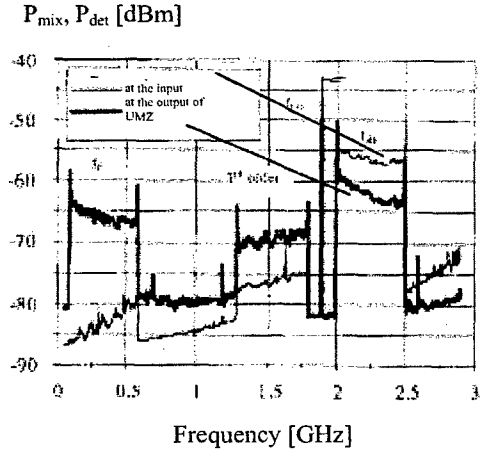

Fig. 24 Power spectra of detected signals with and without UMZ

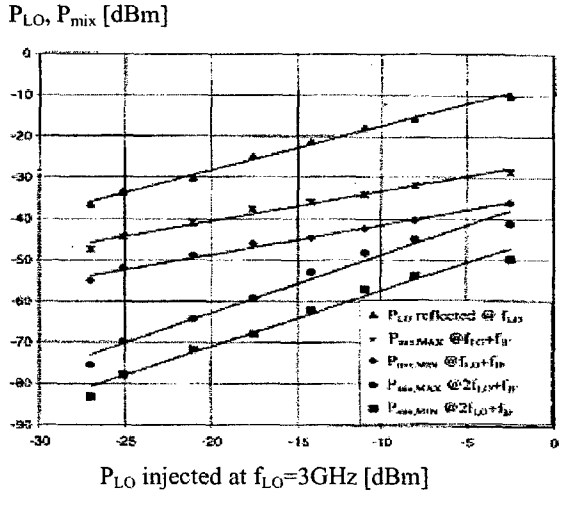

Fig.25 Levels of first and second harmonic mixing as a function of P_{LO}, m=25%(MIN), and m=75%(MAX)

4.4. EXPERIMENTAL RESULTS WITH PD

Investigating the frequency conversion, a PD was illuminated by a DFB laser according to [10]. The LO signal was fed to the PD through a wide-band circulator or a directional coupler separating the LO input and the RF output. No amplifier was used to avoid additional nonlinearities.
Fig. 25 shows the first and second harmonic mixing of f_{IF} and f_{LO} frequencies as a function of the injected LO power measured by a spectrum analyzer. The LO frequency was f_{LO}=3GHz while the optical intensity was modulated by f_{IF}=150MHz. The driving LO signal reflected at the PD is shown as well. A slight saturation effect is observed at P_{LO} close to 0dBm and a proportional increase of the mixing products is shown for greater optical modulation depth (OMD). Results of Fig. 25 demonstrate the interest of exploring the generation of second or higher harmonics for mixing purposes. It can find applications in systems where the LO is received from a remote site. Using subharmonically pumped mixing, only the subharmonic of the LO signal has to be transmitted.

4.5. COMPARISON OF THE TWO METHODS

The principle of the frequency conversion is different in the presented methods. In the first case, the f_{LO} and f_{RF} signals are optically converted by FM, mixed by UMZ, and transmitted. Applications are at the emission side of a fiber-optic link. In the second case, mixing is realized at the reception of the optical link. Only the frequency f_{IF} is transmitted by optical IM.

5. Summary

In this notes a short recapitulation of optical-microwave frequency conversion techniques was given. Optical-microwave signal processing and optical-microwave mixing is one of the most important fields of research regarding todays and future optical-wireless networks and local area networks.

We analyzed a wide spectrum of potential solutions depending on up- or down-conversion and on different device structures, such as MESFETs, p-i-n diodes, unbalanced Mach-Zehnder Interferometric modulators.

On the basis of the widespread references it is possible to make further investigations in the field.

6. References

[1] S.Malone, A.Paolella, P.R. Herczfeld, T.Berceli: "MMIC Compatible Lightwave-Microwave Mixing Techniques.", *IEEE MTT-S Digest* 1992

[2] T.Berceli: "Dynamic Properties of Optical-Microwave Mixing Processes Utilizing FET Devices", *IEEE Transactions on Microwave Theory and Techniques*, Vol. 43, No.9, September 1995

[3] A.Paolella, S.Malone, T.Berceli, P.R.Herczfeld: "MMIC Compatible Lightwave-Microwave Mixing Technique", *IEEE Transactions on Microwave Theory and Techniques*, Vol. 43, No.3, March 1995

[4] T.Berceli: "New methods for subcarrier type optical reception applying new single sideband optical-microwave mixers", *IEEE MTT-S Digest* 1994

[5] T.Berceli, B.Cabon, A.Hilt, A.Ho-Quoc, É.Pic, S.Tedjini: "Dynamic Characterization of Optical-Microwave Transducers", *IEEE MTT-S Digest* 1995

[6] C.P.Liu, Y.Betser, A.J.Seeds, D.Ritter, A.Madjar: "Optoelectronic Mixing in Three-Terminal InP/InGaAs Heterojunction Bipolar Transistors", *IEEE*

[7] T.Berceli, G.Járó: "A New Optical-Microwave Double Mixing Method", *IEEE* 1998

[8] C.P.Liu, A.J.Seeds, D.Wake: "Two-Terminal Edge-Coupled InP/InGaAs Heterojunction Phototransistor Optoelectronic Mixer", *IEEE Microwave and Guided Wave Letters*, Vol. 7, No.3, March 1997

[9] Lu Chao, Chen Wenyue, J. Fu Shiang: "Photonic Mixers and Image-Rejection Mixers for Optical SCM Systems", *IEEE Transactions on Microwave Theory and Techniques*, Vol. 45, No.8, August 1997

[10] G.Maury, A.Hilt, T.Berceli, B.Cabon, A.Vilcot: "Microwave-Frequency Conversion Methods by Optical Interferometer and Photodiode", *IEEE Transactions on Microwave Theory and Techniques*, Vol. 45, No.8, August 1997

[11] A.S.Daryoush, K.Sato, K.Horikawa, H.Ogawa: "Efficient Optoelectronic Mixing at Ka-Band Using a Mode-Locked Laser", *IEEE Microwave and Guided Wave Letters*, Vol. 9, No.8, August 1999

[12] H.Ogawa, Y.Kamiya: "Fiber-Optic Microwave Transmission Using harmonic Laser Mixing, Optoelectronic Mixing, and Optically Pumped Mixing", *IEEE Transactions on Microwave Theory and Techniques*, Vol. 39, No.12, December 1991

[13] H.Kamitsuna, H.Ogawa: "Monolithic Image Rejection Optoelectronic Up-Converters That Employ the MMIC Process", *IEEE 1993 Microwave and Millimeter-Wave Monolithic Circuits Symposium*, 1993

[14] A.Madjar, P.R.Herczfeld, A.Paolella: "Analytical Model for Optically Generated Currents in GaAs MESFETs", *IEEE Transactions on Microwave Theory and Techniques*, Vol. 40, No.8, August 1992

[15] H.Ogawa, Y.Kamiya: "Fiber-Optic Microwave Transmission Using Harmonic Modulation and Optoelectronic Mixing/Optically Pumped Mixing", *IEEE MTT-S Digest*, 1991

[16] K.Matsui, E.Suematsu, T.Takenaka, H.Ogawa: "A One-Chip Integrated Optical/RF Transducer Using a HEMT Optomicrowave Mixer and a Slot Antenna" *IEEE MTT-S Digest*, 1994